Dual-circularly-polarized balanced-fed dielectric rod antenna for 60-GHz point-to-point wireless communication

Dual-Circularly-Polarized Balanced-Fed Dielectric Rod Antenna for 60-GHz Point-to-Point Wireless Communication

M. W. Rousstia (1) and M. H. A. J. Herben (2)
Dept. of Electrical Engineering, Eindhoven University of Technology, P.O. Box 513, 5600 MB Eindhoven, The Netherlands, Email: 1: m.w.rousstia@tue.nl, 2: m.h.a.j.herben@tue.nl

Abstract

The design of a dual-circularly-polarized balanced-fed dielectric rod antenna for 60-GHz point-to-point communication is described and realized. The measured gain and axial ratio are 15dBi and below 0.5dB, respectively.

Introduction

In this work, a high-performance dielectric rod antenna with an optimized dielectric shape for high gain is designed. This high-gain antenna has relative small lateral dimensions and a less-complex structure compared to the design in [1] and [2]. These advantages allow more freedom to add more features, such as dual circular polarization. This dual circular polarization can be used for duplex communication and provides rotational freedom while promoting spectral efficiency. Moreover, for smaller dimension, this antenna can obtain better gain and axial ratio bandwidth than what is reported in [3]. This 60-GHz antenna can be efficiently used for high data rate point-to-point wireless communication in consumer, industrial, and automotive applications.

Design methodology

The dielectric rod is designed to obtain high radiation performance. The detailed dimensions of the rod are depicted in Figure 1(a). This rod will be fed by a patch antenna. The tapered section is to reduce the Side Lobe Level (SLL), and the uniform section is to produce maximum gain. The maximum end-fire radiation is obtained by adjusting the length of those sections. The diameter of the rod supports an HE_{11} hybrid mode if it meets the following relationship

$$D_\lambda \cong \frac{3}{\varepsilon_r^{3/2}\sqrt{1+2L_\lambda}} + 0.2\,, \qquad (1)$$

where D_λ and L_λ are the diameter and total length of the rod in terms of free-space wavelength, respectively.

TPX or polymethylpentene is the material for the dielectric rod. The diameter of the rod base is made large to have sufficient surface area for strong adhesion. Note that the thickness of this rod base should not be larger than 0.16λ. Otherwise, the realized gain will deteriorate.

In Figure 1(b), a quadrature hybrid coupler excites the patch antenna (dashed line) via electromagnetic coupling to the upper layer. This coupler acts as a 3dB power divider with a phase difference of 90°. This phase difference causes the patch to radiate circular polarization. The two arms should be electrically far from the edge of the patch to maintain the polarization purity of the patch radiator. The square patch antenna is used to ensure identical performances for both resulting polarization senses. Two layers of Liquid Crystal Polymer (LCP) laminate are used in this design.

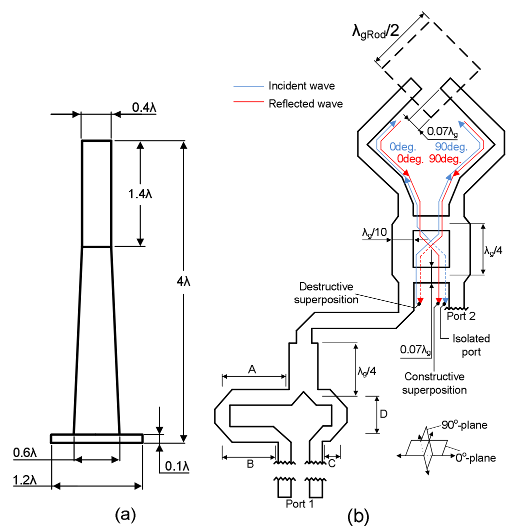

Figure 1: (a) Dimensions of the dielectric rod, (b) the balun, quadrature hybrid coupler, and patch antenna. Illustration of the essential wave paths with their relative phases is provided in coloured lines.

Many millimetre-wave band RFIC's and RF packages have differential signal interfaces. Hence, a balanced-fed input interface to the antenna system is required. The wideband balun is used here to convert the differential to single-ended signal. To design a proper balun at the frequency of interest, the condition for phase contribution from balun dimensions, i.e. A+B+D = 2C+D+180°, should be fulfilled, as illustrated in Figure 1(b). The impedance conversion from 100 to 50 Ω (or vice versa) is performed by the λ/4 transformer.

The design and simulation in this work are analyzed using a full-wave EM simulator, namely CST Microwave Studio and Design Studio.

Scattering parameters

The scattering parameters (S-parameters) of the antenna system are described in this section. The preparation for the measurement is first explained. To feed the antenna system, 60-GHz RPC-1.85 connectors are utilized. The Thru-Reflect-Line (TRL) calibration has been performed before the measurement. For that purpose, it is necessary that RPC connectors with uniform impedance profiles are used. This can be checked using Time Domain Reflectometry (TDR) measurement technique. With the TRL calibration, the influences of microvia, RPC connector and transmission line are de-embedded.

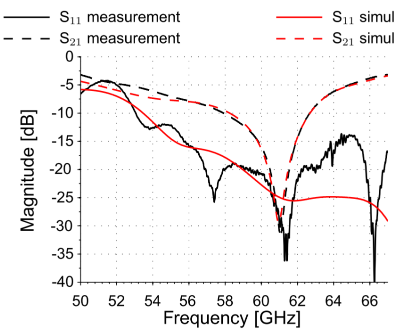

Figure 2: Scattering parameters of the antenna system without the balun.

First the measurement of the S-parameters is performed for the system without the balun. In Figure 2, it can be seen that the measured and simulated results are in a good agreement. From S_{11} curves, it can be seen that the (-10dB) impedance bandwidth of the antenna system is quite broad and spans from 53 GHz up to beyond 67 GHz. On the contrary, the (-20dB) port-to-port isolation bandwidth (S_{21}) is relatively narrow, which is around 1.1 GHz. The scattering parameters are thus interchanged as illustrated in Figure 1(b) and are attributed to the existence of the coupler.

The mismatch at the input of the antenna is reflected back at both arms. Knowing that the waves in each arm have 90° phase difference, the reflected waves that are going to the other port are constructively added whereas the other waves that are going to the exciting port are destructively added. On that account, for a proper hybrid coupler design, S_{21} herein is associated with the resonance of the antenna whereas S_{11} is basically the mutual coupling of the two arms. Hence, the antenna resonance occurs approximately at 61 GHz, and the antenna's (-20dB) isolation bandwidth is 1.1 GHz.

The next step is to perform the measurement of the antenna system with the balun. Consequently, full 4-port measurement of single-ended lines is performed for two differential ports. A general formula to convert the single-ended S-parameters to differential S-parameters is given in the following:

$$S_{MNij} = \frac{1}{2}\left[\left\{s_{(2i-1)(2j-1)} - (-1)^N \cdot s_{(2i-1)(2j)}\right\}\right] - \frac{1}{2}\left[(-1)^M \cdot \left\{s_{(2i)(2j-1)} - (-1)^N \cdot s_{(2i)(2j)}\right\}\right], \quad (2)$$

where M=3 corresponds to ***C***ommon mode, N=4 corresponds to ***D***ifferential mode. i and j are the port numbers of the differential port.

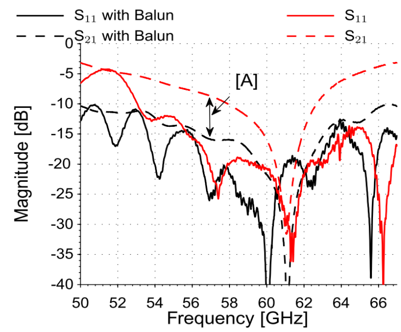

Figure 3: Comparison of scattering parameters of the antenna with (in black) and without (in red) the balun. The gap [A] indicates the contributed loss from the transmission line section.

The measured S-parameters of the whole structure depicted in Figure 1(b) are displayed in Figure 3. Again, the results for the system without the balun are appended here for comparison. It can be seen that the inclusion of the balun in the system does not significantly influence the antenna performance, i.e. antenna resonance.

The RPC connectors are used to feed the antenna system. Hence for measurement convenience, longer differential lines (see Figure 1(b) for port 1) are used to provide more space to attach those connectors to the laminate. As a result, a gap [A] in Figure 3 is basically the loss contributed by that longer line section.

Radiation pattern

The antenna system is designed to have circular polarization. The radiation measurement is thus performed by rotating the linearly polarized horn antenna at 0°, 90°, and 45° positions. From post-processing of the measured data, the realized gain and axial ratio (AR) of the antenna can be obtained. Its polarization sense can be attained from the simulator.

Another important aspect in this measurement is the phase center of the dielectric rod antenna. This phase center can be defined by means of the simulator and is found to be at a height of 1.7λ. If the antenna is rotated around the phase center, the far-field phase remains constant over the main beam in both principle planes.

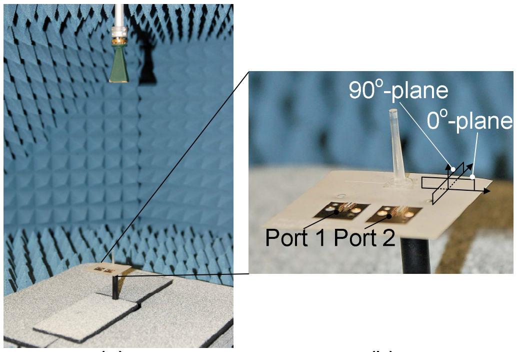

(a) (b)

Figure 4: (a) 60-GHz anechoic chamber and (b) dielectric rod antenna.

In Figure 4, the measurement facility and manufactured dielectric rod antenna are depicted. It can be seen at the top that the horn antenna is used for the measurement of the radiation pattern and at the bottom the manufactured dielectric rod antenna is positioned. In this measurement, the antenna system without the balun is used.

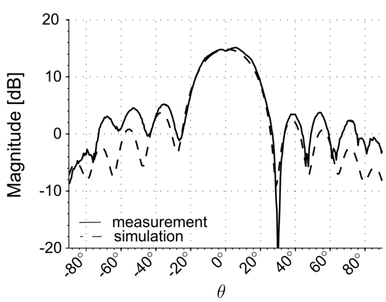

(a) Co-polarization

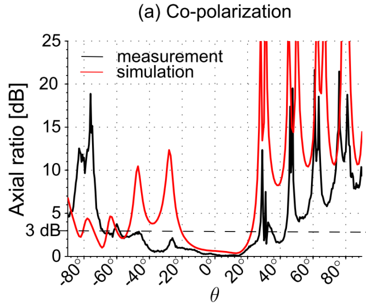

(b) Axial ratio

Figure 5: (a) Co-polarization pattern and (b) axial ratio in the 0°-plane at 61 GHz.

From Figure 5, it is clear that the shapes of the measured simulated co-polar pattern and *AR* pattern agree with the simulated ones. Also the measured antenna gain is as simulated, but the measured *AR* is slightly better than the simulated one. The better measured *AR* than simulated *AR* in the main lobe direction results in a slightly better gain.

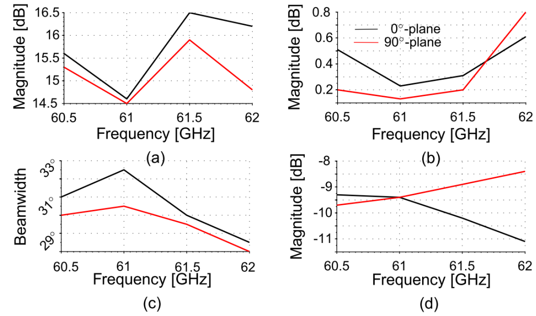

Figure 6: Measured antenna performances over the frequency band of interest. (a) Co-polarization gain, (b) Axial ratio, (c) 3dB beamwidth, and (d) SLL.

In Figure 6, the performance of the dielectric rod antenna for the antenna's (-20dB) isolation bandwidth is summarized for both 0°-plane and 90°-plane. It can be observed that the obtained gain is around 15 dBi. The *AR* is below 0.5 dB. The 3dB beamwidth for both principle planes is similar over the frequency band, showing the symmetry property of the rod's radiation pattern. The sidelobe level is measured to be around -9.5 dB.

Conclusions

The dielectric rod antenna with dual circular polarization and balanced feed line has been designed, manufactured, and measured. The resonance peak occurs around 61 GHz. 15dBi circularly-polarized antenna gain and wide 3dB *AR* bandwidth are realized. The port-to-port (-20dB) isolation bandwidth is 1.1 GHz. This high port-to-port isolation of the antenna enables bi-directional communication with reduced complexity of the RF front-end devices, e.g. it avoids the use of the duplex filter or a switch. Further, the antenna structure is easy and low cost to manufacture and is suitable for the short-range point-to-point communication applications.

Acknowledgement

The authors would like to thank A.C.F. Reniers for the valuable support in the measurement.

References

1. M. Al Henawy et al., *2010 Proceedings of the Fourth European Conference on Antennas and Propagation (EuCAP)*, April 2010, pp. 1-5.
2. N. Caillet et al., *2010 Proceedings of the Fourth European Conference on Antennas and Propagation (EuCAP)*, April 2010, pp. 1-5.
3. K.-C. Huang et al., *IEEE Transactions on Antennas and Propagation*, vol. 54, Jan. 2006, pp. 297-300.